

Air-guided photonic-crystal-fiber pulse-compression delivery of multimewatt femtosecond laser output for nonlinear-optical imaging and neurosurgery

Aleksandr A. Lanin, Il'ya V. Fedotov, Dmitrii A. Sidorov-Biryukov, Lyubov V. Doronina-Amitonova, Olga I. Ivashkina et al.

Citation: *Appl. Phys. Lett.* **100**, 101104 (2012); doi: 10.1063/1.3681777

View online: <http://dx.doi.org/10.1063/1.3681777>

View Table of Contents: <http://apl.aip.org/resource/1/APPLAB/v100/i10>

Published by the [American Institute of Physics](#).

Related Articles

A wireless handheld probe with spectrally constrained evolution strategies for diffuse optical imaging of tissue
Rev. Sci. Instrum. **83**, 033108 (2012)

Synchronization analysis of voltage-sensitive dye imaging during focal seizures in the rat neocortex
Chaos **21**, 047506 (2011)

Photonic-crystal-fiber platform for multicolor multilabel neurophotonic studies
Appl. Phys. Lett. **98**, 253706 (2011)

Multimodal coherent anti-Stokes Raman spectroscopic imaging with a fiber optical parametric oscillator
Appl. Phys. Lett. **98**, 191106 (2011)

Noninvasive, in vivo imaging of the mouse brain using photoacoustic microscopy
J. Appl. Phys. **105**, 102027 (2009)

Additional information on *Appl. Phys. Lett.*

Journal Homepage: <http://apl.aip.org/>

Journal Information: http://apl.aip.org/about/about_the_journal

Top downloads: http://apl.aip.org/features/most_downloaded

Information for Authors: <http://apl.aip.org/authors>

ADVERTISEMENT

NEW!

iPeerReview
AIP's Newest App



**Authors...
Reviewers...**

**Check the status of
submitted papers remotely!**



Air-guided photonic-crystal-fiber pulse-compression delivery of multimewatt femtosecond laser output for nonlinear-optical imaging and neurosurgery

Aleksandr A. Lanin,¹ Il'ya V. Fedotov,^{1,2} Dmitrii A. Sidorov-Biryukov,¹ Lyubov V. Doronina-Amitonova,^{1,2} Olga I. Ivashkina,^{2,3} Marina A. Zots,^{2,3} Chi-Kuang Sun,⁴ F. Ömer Ilday,⁵ Andrei B. Fedotov,^{1,2} Konstantin V. Anokhin,^{2,3} and Aleksei M. Zheltikov^{1,2,6,a)}

¹Physics Department, International Laser Center, M.V. Lomonosov Moscow State University, Moscow 119992, Russia

²Department of Neuroscience, Kurchatov National Research Center, Moscow, Russia

³P.K. Anokhin Institute of Normal Physiology, Russian Academy of Medical Sciences, Moscow, Russia

⁴Graduate Institute of Photonics and Optoelectronics and Department of Electrical Engineering, National Taiwan University, Taipei 10617, Taiwan

⁵Department of Physics, Bilkent University, Cankaya, Ankara 06800, Turkey

⁶Department of Physics and Astronomy, Texas A&M University, College Station, Texas 77843, USA

(Received 9 October 2011; accepted 5 November 2011; published online 6 March 2012)

Large-core hollow photonic-crystal fibers (PCFs) are shown to enable a fiber-format air-guided delivery of ultrashort infrared laser pulses for neurosurgery and nonlinear-optical imaging. With an appropriate dispersion precompensation, an anomalously dispersive 15- μm -core hollow PCF compresses 510-fs, 1070-nm light pulses to a pulse width of about 110 fs, providing a peak power in excess of 5 MW. The compressed PCF output is employed to induce a local photodisruption of corpus callosum tissues in mouse brain and is used to generate the third harmonic in brain tissues, which is captured by the PCF and delivered to a detector through the PCF cladding. © 2012 American Institute of Physics. [doi:10.1063/1.3681777]

Rapidly developing ultrafast laser technologies offer a vast arsenal of solutions and instruments for life sciences. Femtosecond light pulses are showing their utility as a powerful tool for high-resolution bioimaging,^{1–3} intracellular nanosurgery,⁴ laser ophthalmology,^{5,6} targeted cell transfection,⁷ axotomy,⁸ all-optical histology,⁹ targeted action on subsurface cortical blood vessels,¹⁰ and cell fusion.¹¹ While experiments with free-beam ultrashort laser pulses interacting with bio-objects show much promise for diversified life-science applications, such as multiphoton spectroscopy on slices of biotissues,^{1–3} implementation of these approaches in the endoscopic mode, which is often needed for *in vivo* work, faces several fundamental challenges. Standard optical fibers, used for the delivery of ultrashort pulses in the endoscopic mode, tend to give rise to dispersion-induced pulse stretching and impose severe limitations on the laser fluence, which needs to be kept below the fiber damage threshold. In the nano and picosecond ranges of pulse widths, several attractive solutions have been demonstrated using hollow-core photonic-crystal fibers (PCFs),¹² enabling the fiber delivery of high-energy nanosecond¹³ and picosecond¹⁴ laser pulses for a variety of biophotonic and biomedical applications.¹⁵ For femtosecond pulses with relatively low peak powers, typically employed for multiphoton absorption and coherent Raman imaging, the fiber-delivery problem for the endoscopic format of *in vivo* work can often be resolved by using soliton regimes of pulse propagation in hollow-¹⁶ and solid-core¹⁷ PCFs, as well as low-dispersion, low-nonlinearity

air-guided modes in this class of fibers.^{18–20} Femtosecond laser surgery, however, requires an adequate level of laser energy, posing additional serious problems for fiber delivery related to fiber damage by laser radiation.

Here, we show that large-core hollow PCFs operating in the pulse-compression mode can enable a fiber-format air-guided delivery of ultrashort infrared laser pulses for neurosurgery applications. We demonstrate that, with an appropriate dispersion precompensation, a 15- μm -core hollow PCF can compress stretched 510-fs, 1070-nm laser pulses to a pulse width of about 110 fs, providing a peak power in excess of 5 MW. In the experiments presented here, the compressed PCF output is employed to induce a local photodisruption of corpus callosum tissues in mouse brain and is used to generate the third harmonic in brain tissues with backward third-harmonic delivery through the PCF cladding.

The hollow-core PCF used in our experiments includes a periodically structured hexagonal-lattice photonic-crystal cladding and an air-filled 15- μm -diameter hollow core, formed by the omission of 19 fiber-structure elements in the central part of the waveguide. Low-loss light guidance in a fiber with such a design is supported by the photonic band gaps (PBGs) of the periodically structured cladding, which translate into fiber transmission bands.²¹ The structure of the hollow PCF used in our experiments is designed to provide low-loss transmission within the band centered at 1060 nm, suggesting attractive solutions for the fiber delivery of ytterbium laser pulses (cf. the dashed and dashed-dotted lines in Fig. 1(a)). In our experiments, 140-fs ytterbium-laser pulses were transmitted through a 1-m piece of such a fiber with minimal spectral distortions and a loss below 0.05 dB/m.

^{a)}Author to whom correspondence should be addressed. Electronic mail: zheltikov@phys.msu.ru.

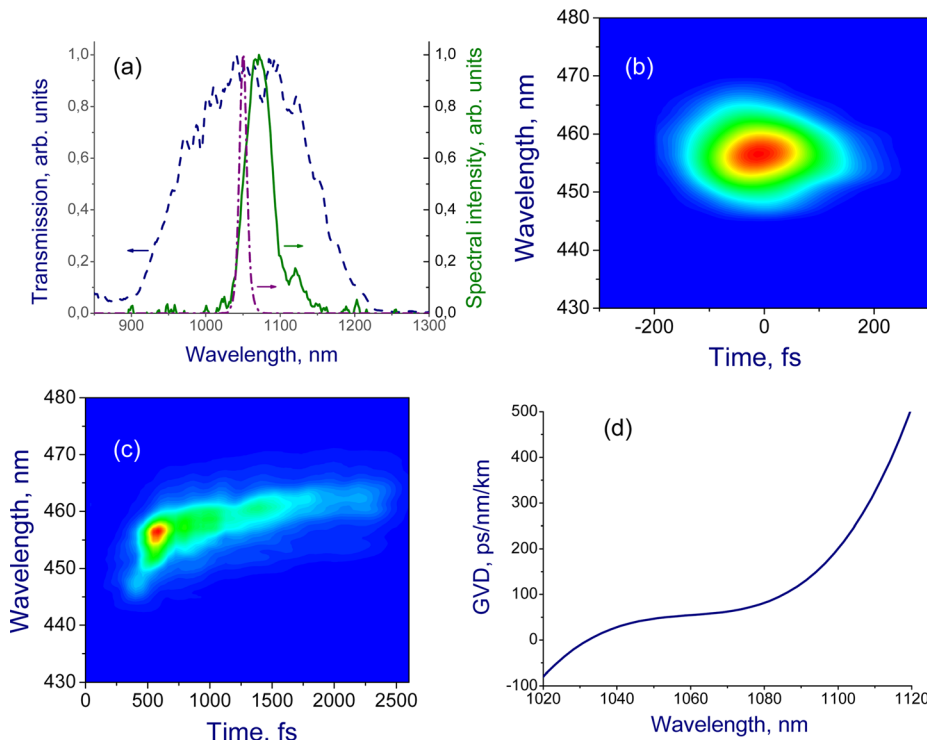


FIG. 1. (Color online) (a) Transmission spectrum of the hollow PCF (dashed line), the spectrum of the ytterbium laser output (dash-dotted line), and the spectrum of the OPA output (solid line). (b) and (c) XFROG traces of the probe laser pulse measured at the input (b) and output (c) of a 20-cm piece of a hollow PCF with a hexagonal-lattice photonic-crystal cladding and a core diameter of $15\ \mu\text{m}$. (d) The spectral profile of the fiber GVD as retrieved from the XFROG traces.

Due to the high damage threshold and low nonlinearity of the hollow fiber core, laser pulses with a high peak power can be transmitted through a fiber with such a design.¹⁴ Strong waveguide dispersion of hollow PCFs, however, gives rise to the stretching of ultrashort laser pulses, limiting the utility of fiber-based delivery in a broad variety of nonlinear-optics-based biomedical applications. Here, we seek the solution to this problem by exploiting an important general property of the group-velocity dispersion (GVD) of PBG-guided hollow-PCF modes, which tends to vanish at a median point of the PCF transmission band, becoming anomalous toward longer wavelengths. To visualize this tendency, we use a 100-fs, 1070-nm output (the solid line in Fig. 1(a)) of an optical parametric amplifier (OPA) pumped by amplified pulses of a mode-locked Ti: sapphire laser. Figures 1(b) and 1(c) present the cross-correlation frequency-resolved optical gating (XFROG) traces²² recorded with the use of a 0.5-mm-thick BBO crystal and 790-nm, 80-fs reference pulses, delivered by the Ti: sapphire laser, for the 1070-nm OPA output with an initial chirp of $1500\ \text{fs}^2$ before and after the hollow PCF. As can be seen from these measurements, the fiber dispersion tends to stretch 100-fs light pulses to an output pulse width of 490 fs. The fiber GVD retrieved from these XFROG traces (Fig. 1(d)) is indeed anomalous, suggesting the possibility of simple schemes of dispersion pre-compensation for the shortest pulse width at the PCF output.

For the precompensation of fiber dispersion, tunable chirp was imposed on laser pulses with a stack of silica plates. An XFROG trace of an OPA pulse stretched by such a dispersion-precompensation scheme to a pulse width of approximately 510 fs is shown in Fig. 2(a). The temporal envelope and the chirp of the stretched OPA pulses retrieved from the XFROG traces are presented in Fig. 2(b). Pulse stretching is dominated by a linear chirp, which is estimated

as $6540\ \text{fs}^2$. The spectrum of the stretched pulses retrieved from the XFROG traces (the solid line in Fig. 2(c)) closely follows the directly measured spectrum (filled circles in Fig. 2(c)). The spectral phase of these pulses, also retrieved from XFROG measurements (the dashed line in Fig. 2(c)), visualizes the parabolic phase profile introduced by pulse stretching.

The stretched light pulses with an energy of $0.5\ \mu\text{J}$ are coupled into a 20-cm section of hollow-core PCF by a micro-objective with a numerical aperture of 0.2. For the chosen parameters of the fiber and laser pulses, the B integral, $B = 2\pi\lambda^{-1} \int n_2 I(z) dz$, where λ is the wavelength, n_2 is the nonlinear refractive index, and $I(z)$ is the field intensity, is less than unity, allowing effects related to the nonlinear phase shift to be avoided. The XFROG trace of the PCF output (Fig. 2(d)) and its temporal phase profile (the dashed line in Fig. 2(e)) indicate that most of the linear part of the input chirp has been compensated by PCF dispersion, restoring the initial pulse width of about 110 fs and providing a peak power of about 5 MW. The temporal envelope of the PCF output retrieved from the XFROG trace is shown by the solid line in Fig. 2(e). The spectrum and the spectral phase of the PCF output (Fig. 2(f)) confirm that the nonlinear-optical effects are weak, which is consistent with the estimate for the B integral. The noncompensated phase, seen in Figs. 2(e) and 2(f), is dominated by high-order dispersion of the hollow PCF.

The compressed PCF output was collimated and then focused on a slice of a mouse brain tissue with a pair of aspherical lenses with a numerical aperture of 0.55 (Fig. 3(a)). Focusing to a beam diameter of $3\text{--}5\ \mu\text{m}$ yielded a laser field intensity of $30\text{--}70\ \text{TW}/\text{cm}^2$ and a laser fluence of $3\text{--}7\ \text{kJ}/\text{cm}^2$. This level of fluence is more than two orders of magnitude higher than the breakdown threshold of a

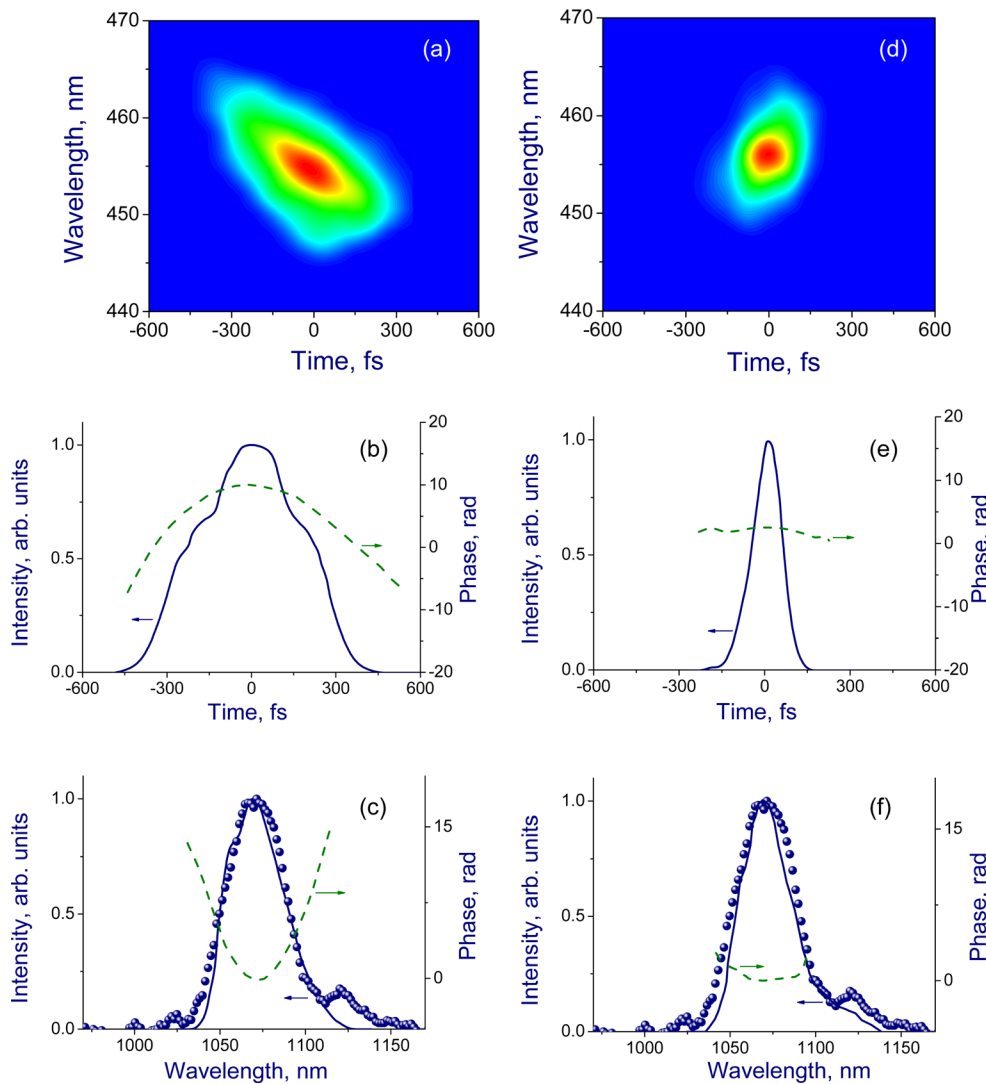


FIG. 2. (Color online) Characterization of laser pulses at the input (a)–(c) and at the output (d)–(f) of the hollow PCF: (a) and (d) XFROG traces of the input (a) and output (d) pulses; (b) and (e) temporal envelopes (solid lines) and chirps (dashed lines) of the input (b) and output (e) pulses; (c) and (f) measured spectra (filled circles), spectra retrieved from the XFROG traces (solid lines), and the spectral phases (dashed lines) of the input (c) and output (f) pulses.

transparent wide-gap dielectric, such as fused silica.²³ For biotissues, laser fluences and field intensities in this range are sufficient for a broad range of biomedical applications, including multiphoton microscopy,^{1–3} high-performance laser surgery,⁴ laser ophthalmology,^{5,6} optical histology,⁹ cell-membrane photoperforation,²⁴ and photostimulated calcium-response stimulation.²⁵ Figure 3(b) presents an image of the region of photodisruption induced on a slice of a corpus callosum tissue from mouse brain. The 1070-nm laser pulses transmitted through the hollow PCF also provide a pump for third-harmonic generation (THG) in the beam-focus region, enabling high-resolution nonlinear-optical imaging of brain tissues. The third-harmonic signal is collected by the fiber cladding and delivered to the third-harmonic detection (THD) system, consisting of spectral filters and a photomultiplier (Fig. 3(a)). The guidance loss provided by this light-deliver regime at the central wavelength of the third-harmonic signal (357 nm) is below 0.2 dB/m. Due to the low optical nonlinearity of the air filling the hollow PCF core and the low field intensity in the evanescent part of the PCF modes in the PCF cladding, the background third-harmonic signal generated by the high-intensity pump inside the fiber is more than an order of magnitude lower than the third harmonic from the brain tissue.

The sensitivity of THG to ultrafast free-carrier generation by an ultrashort pump pulse²⁶ suggests a promising approach for local detection of photodisruption in biotissues.

In conclusion, we have demonstrated that large-core hollow PCFs enable a fiber-format air-guided delivery of ultrashort infrared laser pulses for neurosurgery applications. With an appropriate dispersion precompensation, an anomalously dispersive 15- μm -core hollow PCF are shown to compress 510-fs, 1070-nm light pulses to a pulse width of about 110 fs, providing a peak power in excess of 5 MW, enabling

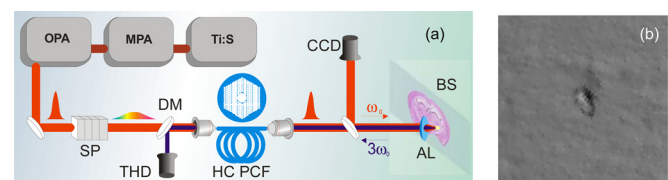


FIG. 3. (Color online) (a) Diagram of laser-induced photodisruption of a brain tissue by ultrashort laser pulses delivered by a hollow PCF: Ti: S, mode-locked Ti: sapphire laser oscillator; MPA, multipass amplifier; OPA, optical parametric amplifier; SP, stack of silica plates; DM, dichroic mirror; HC PCF, hollow-core photonic-crystal fiber; AL, aspheric lens; BS, slice of brain tissue; THD, third-harmonic detection. (b) An image of the region of photodisruption induced by ultrashort laser pulses on a slice of a corpus callosum tissue from mouse brain.

a nonlinear-optical diagnostics and a local photodisruption of brain tissues.

This work was supported in part by the Russian Foundation for Basic Research (projects 11-02-92012, 10-02-91226, and 11-02-92118), the Federal Program of the Russian Ministry of Education and Science (contracts 1130 and 02.740.11.0223), the Seventh European Framework Programme (CROSS TRAP 244068 project) and the Scientific and Technological Research Council of Turkey (TÜBİTAK, project 209T058).

- ¹W. Denk, J. H. Strickler, and W. W. Webb, *Science* **248**, 73 (1990).
- ²W. R. Zipfel, R. M. Williams, and W. W. Webb, *Nat. Biotechnol.* **21**, 1369 (2003).
- ³F. Helmchen and W. Denk, *Nat. Methods* **2**, 932 (2005).
- ⁴K. Koenig, I. Riemann, P. Fischer, and K. H. Halhuber, *Cell. Mol. Biol.* **45**, 195 (1999).
- ⁵T. Juhasz, H. Frieder, R. M. Kurtz, C. Horvath, J. F. Bille, and G. Mourou, *IEEE J. Sel. Top. Quantum Electron.* **5**, 902 (1999).
- ⁶K. König, I. Riemann, and W. Fritzsche, *Opt. Lett.* **26**, 819 (2001).
- ⁷U. K. Tirlapur and K. König, *Nature* **418**, 290 (2002).
- ⁸M. F. Yanik, H. Cinar, H. N. Cinar, A. D. Chisholm, Y. S. Jin, and A. Ben-Yakar, *Nature* **432**, 822 (2004).
- ⁹P. S. Tsai, B. Friedman, A. I. Ifarraguerri, B. D. Thompson, V. Lev-Ram, C. B. Schaffer, C. Xiong, R. Y. Tsien, J. A. Squier, and D. Kleinfeld, *Neuron* **39**, 27 (2003).
- ¹⁰N. Nishimura, C. B. Schaffer, B. Friedman, P. S. Tsai, P. D. Lyden, and D. Kleinfeld, *Nat. Methods* **3**, 99 (2006).
- ¹¹J. X. Gong, X. M. Zhao, Q. R. Xing, F. Li, H. Y. Li, Y. F. Li, L. Chai, Q. Y. Wang, and A. M. Zheltikov, *Appl. Phys. Lett.* **92**, 093901 (2008).
- ¹²P. St. J. Russell, *Science* **299**, 358 (2003).
- ¹³J. Tauer, F. Orban, H. Kofler, A. B. Fedotov, I. V. Fedotov, V. P. Mitrokhin, A. M. Zheltikov, and E. Wintner, *Laser Phys. Lett.* **4**, 444 (2007).
- ¹⁴S. O. Konorov, A. B. Fedotov, O. A. Kolevatova, V. I. Beloglazov, N. B. Skibina, A. V. Shcherbakov, E. Wintner, and A. M. Zheltikov, *J. Phys. D: Appl. Phys.* **36**, 1375 (2003).
- ¹⁵S. O. Konorov, A. B. Fedotov, V. P. Mitrokhin, V. I. Beloglazov, N. B. Skibina, A. V. Shcherbakov, E. Wintner, M. Scalora, and A. M. Zheltikov, *Appl. Opt.* **43**, 2251 (2004).
- ¹⁶A. A. Ivanov, A. A. Podshivalov, and A. M. Zheltikov, *Opt. Lett.* **31**, 3318 (2006).
- ¹⁷L. V. Doronina, I. V. Fedotov, A. A. Voronin, O. I. Ivashkina, M. A. Zots, K. V. Anokhin, E. Rostova, A. B. Fedotov, and A. M. Zheltikov, *Opt. Lett.* **34**, 3373 (2009).
- ¹⁸S.-P. Tai, M.-C. Chan, T.-H. Tsai, S.-H. Guol, L.-J. Chen, and C.-K. Sun, *Opt. Express* **12**, 6122 (2004).
- ¹⁹B. A. Flusberg, J. C. Jung, E. D. Cocker, E. P. Anderson, and M. J. Schnitzer, *Opt. Lett.* **30**, 2272 (2005).
- ²⁰L. V. Doronina-Amitonova, I. V. Fedotov, O. I. Ivashkina, M. A. Zots, A. B. Fedotov, K. V. Anokhin, and A. M. Zheltikov, *Appl. Phys. Lett.* **98**, 253706 (2011).
- ²¹R. F. Cregan, B. J. Mangan, J. C. Knight, T. A. Birks, P. St. J. Russell, P. J. Roberts, and D. C. Allan, *Science* **285**, 1537 (1999).
- ²²G. P. Agrawal, *Nonlinear Fiber Optics*, 4th ed. (Academic, San Diego, 2007).
- ²³M. Lenzner, J. Krüger, S. Sartania, Z. Cheng, Ch. Spielmann, G. Mourou, W. Kautek, and F. Krausz, *Phys. Rev. Lett.* **80**, 4076 (1998).
- ²⁴J. Baumgart, W. Bintig, A. Ngezahayo, S. Willenbrock, H. Murua Escobar, W. Ertmer, H. Lubatschowski, and A. Heisterkamp, *Opt. Express* **16**, 3021 (2008).
- ²⁵N. I. Smith, K. Fujita, T. Kaneko, K. Kato, O. Nakamura, T. Takamatsu, S. Kawata, *Appl. Phys. Lett.* **79**, 1208 (2001).
- ²⁶A. B. Fedotov, S. M. Gladkov, N. I. Koroteev, and A. M. Zheltikov, *J. Opt. Soc. Am. B* **8**, 373 (1991).